

direction bias, and comparison of the reflectivity and rms slope parameters will also be presented at the colloquium.

The association of anomalous scattering behavior and impact parabola features suggests that impact-derived materials are involved. These probably have unique properties among Venus surface materials with respect to their size distribution (a large component of fines?) and possibly with respect to composition or mineralogy. The presence of streaks suggests that wind processes are involved. Under a surface change scenario, the variations in SAR backscatter are suggested to result from redistribution of a layer of loose material, possibly by wind, during the interval between data acquisitions. However, the scale of the observed differences requires large volumes of material to be redistributed over a short period of time. Furthermore, the common occurrence of impact parabola features on the planet indicates that the age of the population of parabolas is probably on the order of tens to hundreds of Ma. It seems unlikely, if these surfaces were vulnerable to such rapid change, that they would retain their distinctive signatures over such a time span.

The viewing geometry hypothesis requires surfaces that contain geometrical elements that favor or diminish backscatter strength, depending on the side from which the surface is observed. The very nearly identical incidence angles (though east- and west-looking), require that the surfaces have a strong asymmetrical component in the east-west direction. The dominant asymmetry in the parabolic features is in the east-west direction (parabolas "open" to the west), so it may be inferred that structures at a smaller scale have an east-west component of asymmetry. Aeolian bedforms (ripples, dunes) are the prime candidates for such structures in the parabola areas. Terrestrial transverse dunes typically have stoss slopes of  $5^{\circ}$ – $10^{\circ}$ , and slip face slopes of  $30^{\circ}$ – $35^{\circ}$ . The absence of the "speckly" returns commonly observed in SAR images of dunes implies that the bedforms responsible for the extensive bright patches contain faces at scales of tens of centimeters to no more than a few tens of meters. The visibility of aeolian bedforms in SAR imagery is known to be highly sensitive to look azimuth, relative to the dominant strike direction of slopes [4]. In the high southern latitudes discussed here, the look azimuth between cycles differed by  $\sim 160^{\circ}$ , which may

further affect the visibility of features. Several difficulties remain with the bedform hypothesis. The large enhancement in backscatter on steep faces should have a corresponding smaller enhancement on the shallow faces. This effect is not observed. The reversal in "sense" of the anomalies is also somewhat inconsistent with bedforms developed within a wind regime dominated by one persistent direction of flow, necessary for such widespread, consistent slope distributions.

References: [1] Arvidson R. E. et al. (1991) *Science*, 252, 270–275. [2] Campbell D. B. et al. (1992) *JGR*, special Magellan issue, in press. [3] Pettengill G. H. et al. (1991) *Science*, 252, 260–265. [4] Blom R. G. (1988) *Int. J. Rem. Sens.*, 9, 945–965.

## N93-14364

CYTHEREAN CRUSTAL BENDING AT SALME DORSA.  
J. Raitala and K. Kauhanen, Department of Astronomy, University of Oulu, Finland.

The horseshoe-like, narrow (100 km wide and 600 km long) Salme Dorsa consists of arcuate ridges and grooves opening south-east on the planitia to the south of Ishtar Terra. Magellan radar data was studied in order to find tectonic style and lithospheric thickness of the area. The Salme ridge belt indicates folding and thrust faulting of surface layers due to compression against the tessera foreland zone. The western edge of Salme Dorsa is scarplike. Most ridges follow the main course of the arc and the overall ridge orientation is north-south while ridges subparallel the arcuate edge. The ridge trend at the northeastern end is northeast-southwest, while the southern part of the horseshoe has more northwestern ridges. The ridge belt has elements of normal compression against the zone. It has widened due to the new ridge formation. As this process repeats itself, the crust also becomes thicker making the topographically high ridge belt act as a load.

The scarp along the western edge of Salme Dorsa indicates that the movement has been to the west or northwest. West of Salme Dorsa the crust has bent due to the load and/or thrust of Salme Dorsa, resulting in a trough outside the scarp. The compressional ridge belt has acted either as a nappe overthrust or as a mere surface load due

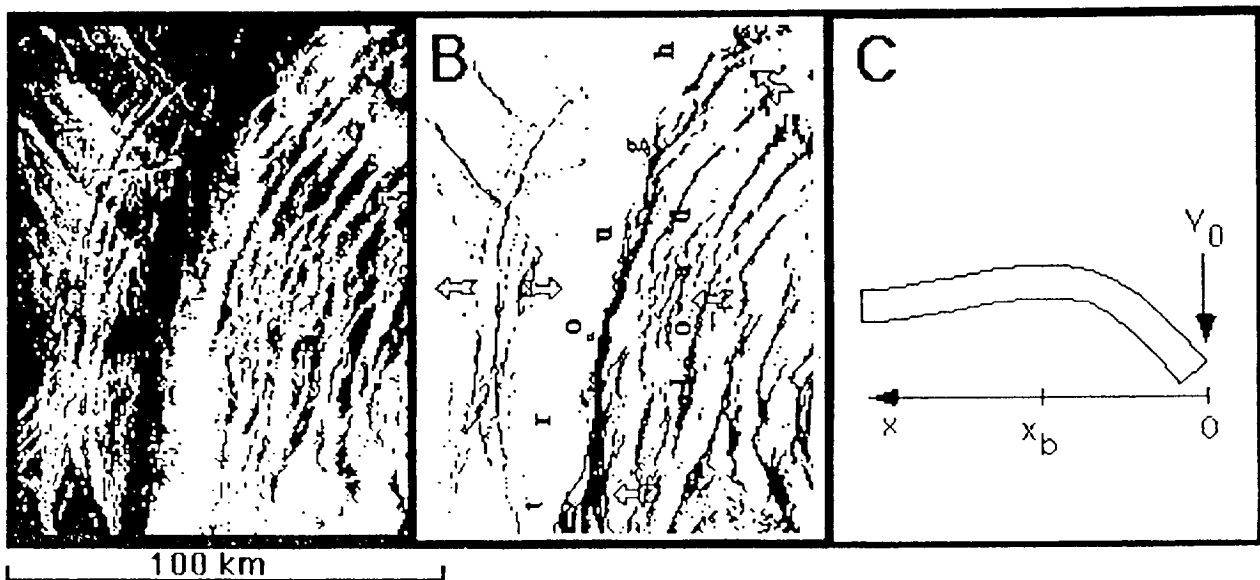


Fig. 1. Radar image of the crustal bending at central Salme Dorsa (a). The load and compression/tension stress system is displayed (b) and modeled with vertical exaggeration (c). The trough depression is next to a surface load and/or compressional massif. Grabens are located on the anticlinal bulge.

to crustal thickening under stress from the east or southeast. Salme Dorsa cuts through the ridges of older Sigrun Fossae. Salme Dorsa has quite a recent border scarp and is obviously relatively young. Interlocking nearby ridge belts indicate repeated compressions.

The trough and bulge west of Salme Dorsa is caused by crustal bending due to the ridge belt load or nappe thrust to the west. Tensional grabens along the crest of the bulge indicate crustal extension. The grabens parallel the ridge belt and trough as gentle arcs that open in the direction of Salme Dorsa on the bulge crest. Elastic deformation of the layered crust and adjoining fracturing of the uppermost brittle surface might be reasonable assumptions. The set of narrow grabens on top of the bulge are due to excess tensile stress in the uppermost brittle layer of the lithosphere. The lack of corresponding troughs, bending, or grabens on the eastern side of the ridge belt may indicate that both the load and the thrust from the east have to be taken into account. The volcanic area inside the Salme Dorsa horseshoe have also weakened the crust on that side.

The elastic layer is confined by the temperature above which the upper mantle has negligible strength [1]. The elastic part of the lithosphere is defined by isotherms 450°C and 650°C and this elastic lithosphere is considerably thinner than the low-attenuation seismic lithosphere. The temperature gradients of 15°C/km [2] and 20°C/km [3] and the surface temperature of 470°C suggest that the lower boundary of the elastic lithosphere is about 12 km or 9 km deep, respectively.

The thickness of the elastic layer is estimated using a flexural approach and a two-dimensional model of a semi-infinite broken elastic lithosphere under a linear load [4] with the only acting force,  $V_0$ , applied vertically to its end, where the bending moment is zero. The only measurable quantity,  $x_b$ , is the distance between the force and the bulge. The equation for the deflection of a plate includes loading of the lithosphere by vertical forces, hydrostatic restoring force, and the position of the bulge. Assuming a basaltic composition for the crust,  $\rho_c = 3000 \text{ kgm}^{-3}$ ,  $E = 0.6 \times 10^{11} \text{ Pa}$  and  $\nu = 0.25$  and using  $\rho_m = 3300 \text{ kgm}^{-3}$ ,  $g = 8.6 \text{ ms}^{-2}$  and  $x_b = 50 \text{ km}$  we find  $h \approx 2.9 \text{ km}$  for the elastic thickness of the lithosphere.

Variations in the magnitudes of the vertical or horizontal loads or the bending moment will alter the displacement but will not alter the position of the top of the bulge. Changes in the model, application of a horizontal force or a bending moment, will have more dramatic effects on the distance of the bulge and the lithospheric thickness. If a bending moment is assumed, the thickness of the lithosphere increases due to the increasing effect on plate curvature. The free edge boundary of our model is justified by volcanic activity that has weakened the lithosphere. Both a three-dimensional model and a continuous elastic plate model will reduce the elastic thickness. Allowing a bending moment to act upon the plate end, the elastic thickness of the lithosphere increases by a factor of 2.

The elastically thick lithosphere can support high compressional stresses or fail by faulting rather than buckling. Compressional stress critical to deformation can be estimated [4] to be approximately 0.4 GPa, taking the previous values. The wavelength of the buckling at the critical stress is about 94 km, and is reduced as the stress increases. This value corresponds well to the distance between Salme Dorsa and the bulge, and thus horizontal forces cannot be totally neglected. Recent research has revealed that buckling of the lithosphere can occur at stress levels much less than the elastic strength of the lithosphere [5]. Horizontal forces may have contributed to the buckling but it is difficult to find out which one of the forces has been active for a thickness of the elastic lithosphere of about 3 km. If both forces are allowed [6], the thickness of this layer of the lithosphere is slightly increased to 3.1 km.

**Summary:** The Salme ridge belt can be interpreted as being the leading edge of a venusian crustal unit that moved against the highland foreland unit. It is indicative of a compressional zone, with a thrust front facing west. The Salme Dorsa ridge belt with adjoining structures is an evident indication of lateral stresses and adjoining crustal movements on Venus. It supports the idea of southeast compression against and over the foreland planitia, which has bent under the load and/or lateral stress, resulting in trough and bulge formation in front of the ridge belt. The origin of the driving force for the movements remains masked. Laima Tessera is located in the direction from which the thrust is thought to apply [7] but there are no appropriate candidates for a rift zone although a thrust from the southeast would be in good agreement with structures of Laima Tessera. The temperature gradient [2] suggests that the lithosphere is approximately 12 km thick, while its elastic layer is approximately 3 km thick based either on the load-induced flexure model or on the compressional buckling model.

**References:** [1] Kirby S. H. (1983) *Rev. Geophys. Space Phys.*, 21, 1528–1538. [2] Smrekar S. E. and Solomon S. C. (1992) *Workshop on Mountain Belts on Venus and Earth*, 35–37. [3] Solomon S. C. and Head J. W. (1989) *LPSC XX*, 1032–1033. [4] Turcotte D. L. and Schubert G. (1982) *Geodynamics: Applications of Continuum Physics to Geological Problems*, Wiley, New York, 450 pp. [5] Stephenson R. A. and Cloetingh S. A. P. L. (1991) *Tectonophysics*, 188, 27–37. [6] McAadoo D. A. and Sandwell D. T. (1985) *JGR*, 90, 8563–8569. [7] Raitala J. and Tormanen T. (1990) *Earth Moon Planets*, 49, 57–83.

## N93-14365

**COMPUTER SIMULATIONS OF COMET- AND ASTEROIDLIKE BODIES PASSING THROUGH THE VENUSIAN ATMOSPHERE—PRELIMINARY RESULTS ON ATMOSPHERIC AND GROUND SHOCK EFFECTS.** D. Roddy<sup>1</sup>, D. Hatfield<sup>2</sup>, P. Hassig<sup>2</sup>, M. Rosenblatt<sup>2</sup>, L. Soderblom<sup>1</sup>, and E. De Jong<sup>3</sup>, <sup>1</sup>U.S. Geological Survey, Flagstaff AZ, USA, <sup>2</sup>California Research & Technology, Chatsworth CA, USA, <sup>3</sup>Jet Propulsion Laboratory, Pasadena CA, USA.

We have completed computer simulations that model shock effects in the venusian atmosphere caused during the passage of two comelike bodies 100 m and 1000 m in diameter and an asteroidlike body 10 km in diameter. Our objective is to examine hypervelocity-generated shock effects in the venusian atmosphere for bodies of different types and sizes in order to understand (1) their deceleration and depth of penetration through the atmosphere and (2) the onset of possible ground-surface shock effects such as splotches, craters, and ejecta formations. The three bodies were chosen to include both a range of general conditions applicable to Venus as well as three specific cases of current interest.

These calculations use a new multiphase computer code (DICE-MAZ) designed by California Research & Technology for shock-dynamics simulations in complex environments. The code has been tested and calibrated in large-scale explosion, cratering, and ejecta research. It treats a wide range of different multiphase conditions, including material types (vapor, melt, solid), particle-size distributions, and shock-induced dynamic changes in velocities, pressures, temperatures (internal energies), densities, and other related parameters, all of which were recorded in our calculations. DICE-MAZ is especially useful in our Venus study because of the advance capability in multiphase adaptive zoning and because of the color coding associated with displaying the complex variations in